Design of Dual Band Substrate Integrated Waveguide (SIW) Antenna with Modified Slot for Ka-Band Applications

Saravanan Ramamoorthi Agilesh
Department of Electronics and Communication Engineering, Antennas and Liquid Crystals Research Center, Koneru Lakshmaiah Education Foundation, India
agileshece@gmail.com (corresponding author)

Boddapati T. P. Madhav
Department of Electronics and Communication Engineering, Antennas and Liquid Crystals Research Center, Koneru Lakshmaiah Education Foundation, India
btpmadhav@kluniversity.in

A. Gangadhar
Department of ECE, JNTUK Narsaropet, India
gangadhar.ece@jntukucen.ac.in

Sarada Sowjanya Chintalapati
Department of CSE (DS), Sreyas Institute of Engineering and Technology, India
soujikits@gmail.com

Received: 29 April 2024 | Revised: 10 May 2024 | Accepted:12 May 2024

 DOI: https://doi.org/10.48084/etasr.7620

ABSTRACT

This paper introduces a dual-feed substrate integrated waveguide antenna design with a modified H-Slot (DFH-SIW) for Ka-band 5G applications. In general, 5G base stations operating in Ka-band applications need large bandwidth-based antennas with high gain to solve the problem of path loss and high data capacity. To resonate with an ideal bandwidth at 28/38 GHz, this study proposes a high-gain antenna with a modified H-slot. This study used the CST EM tool to design the proposed antenna model and evaluate and optimize its characteristics. The proposed dual feed antenna has compact dimensions of 12×12×1.2 mm and was constructed on a Roger 5880 substrate with an appropriate permittivity of 2.2 and a minimal loss tangent of 0.0009. The proposed dual-feed antenna showed an ideal reflection coefficient of less than -10dB and a bandwidth of 3.7 GHz and 3.23 GHz at operating frequencies of 28 and 38 GHz, respectively. The proposed design operates at the 28 GHz frequency with 73.2% efficiency and 4.3 dBi gain, and at 38 GHz with 83.68% efficiency and 6.7 dBi gain. This antenna is intended to be used in future 5G wireless networks and has outstanding overall performance in terms of return loss, gain, and wide bandwidth.

Keywords-dual feed; H-slot; Substrate Integrated Waveguide (SIW); 5G

I. INTRODUCTION

As technology advances, there is a growing need for wireless data bandwidth and improved mobile data experience for users, which has led to an increase in the demand for network utilization of the available wireless spectrum. One of the biggest concerns for 5G communications is the bandwidth of the wireless network. The Ka-band of 5G cellular networks operates at the millimeter wave (mmWave) frequency bands of 27 to 40 GHz. The Ka-band mmWave frequency spectrum has attracted the interest of many studies for potential use in 5G networks. Attenuation and absorption by the atmosphere increase with increasing frequency in 5G wireless communication. The losses due to attenuation and free space propagation are both less at the 28 and 38 GHz bands than in the other mmWave bands. Dual-band and multi-band antennas, which have advantages such as small size, easier integration, and lower cost, are expected to become standard for future wireless communications. For this reason, future mmWave wireless communication will likely utilize dual-band broadband antennas.

Several different dual-band antenna designs and types have been proposed. Diverse types of antennas, such as the wide band slot loaded patch antenna [1], the folding rectangular slot and loading C-slot antenna [2], and the Dielectric Resonator Antenna (DRA) slot [3], have been employed in various ways for dual-band operation. Moreover, suggestions for dual-band operation have included the same kind of antennas in various sizes or configurations. These operate using various transmission line types and configurations, such as Substrate Integrated Waveguide (SIW) fed holes [4]. An antenna with two layers and a modified cavity was proposed in [5-7] to achieve directed radiation patterns and resonance throughout the mmWave frequency range. In [8], a dual-band elliptical microstrip antenna with enhanced performance was proposed, employing Rogers RO3010 combined with RO4350B and having a global surface area of 0.754 mm^2. In [9], a single-feed SIW antenna with a slotted cavity was proposed for dual-band mmWave Circular Polarization (CP) applications, operating in two different modes. In [10], a hybrid slotted antenna array with a dielectric resonator had the best gain, but its center frequency was affected and offered the least bandwidth. In [11], a dual-band SIW antenna array topology was proposed, which had a high gain to overcome path loss. This antenna had improved efficiency and provided optimal bandwidth in the upper band but comparatively less bandwidth in the lower band. In [6], a high-gain single-feed dual-band antenna was presented, but it had a nonoptimal bandwidth in the top band. In [12], a dual-band mmWave antenna was presented, having a single element with a two-port MIMO configuration. The impedance matching bandwidth was highly affected due to the complex radiation method. Although the gain increased, it was not able to produce optimal bandwidth.

SIW is an exciting method for addressing antenna design issues such as gain, return loss, bandwidth, and efficiency. In [13], a compact dual-band SIW antenna with optimal gain and bandwidth was introduced, however, although this design satisfied the need for bandwidth, it was highly affected by path loss as it was unable to produce the optimal return loss. The Substrate Integrated Circuits (SICs) theory describes how non-planar structures can be transformed into planar and provides the foundation for SIW [14]. In [15], a high isolation dual-band antenna array was proposed for MIMO applications, which was very compact and provided optimal gain but failed to maintain the optimal bandwidth and reflection coefficient at high data transmission. In [16], a simple dual-band antenna with a modified H-slot was introduced, which maintained the optimal bandwidth and gain but the return loss affected its highest band. In [17-19] various mmWave SIW antennas were reviewed and compared. Slotted SIW antennas can improve bandwidth efficiency, optimal gain, larger bandwidth, return loss, and radiation pattern, among other factors. Simulation findings have shown that antenna gain increases by increasing the number of slots in antenna designs. In [20], a dual-band antenna with a circular cavity-backed slot array was proposed, based on a substrate-integrated waveguide and employing TM 020 for 5G applications. In [11], a dual-band SIW antenna array structure was proposed for use in the frequency ranges 28/38 GHz, using a tight coupling between four miniature quarter-mode SIW cavities to produce an antenna architecture with four unique resonance frequencies. In [21] a compact single-feed dual-band antenna with a rectangular and ring-slotted SIW cavity was designed to provide an ideal radiation pattern. This design used an additional half-wavelength transverse stub added to the microstrip single feed line to reduce crosstalk between the microwave and mmWave signals.

This study proposes a dual-feed SIW antenna design with a modified H-slot configuration to enhance bandwidth and gain and maintain a stable radiation pattern with optimal return loss. Dual-band resonances are created in the proposed antenna due to the availability of an even distribution of modified H-slots that are engraved into the patch along with the substrate-integrated waveguide structure. Using SIW with modified H-slot configurations can provide optimal directional radiation patterns. Radiating apertures are typically found in the other conducting layer in SIW structures, which is typically the ground. The apertures to radiate electromagnetic waves alter the distribution of surface currents and increase the gain of the antenna. The dual feeding mechanism used in the proposed antenna further enhances the bandwidth at the resonance frequencies. A fully grounded plane was used for this design, and the reflection coefficient was found to be less than -10 dB at two different operating frequencies 28/38 GHz.

II. PROPOSED ANTENNA DESIGN

The fundamental design of SIW features a substrate in the center of the metal planes, two rows of periodic holes, and a rectangular waveguide. The proposed SIW antenna was made with a Rogers RT5880 base that had a thickness of 1.2 mm, a dielectric constant of 2.2, a loss tangent of 0.0009, and compact dimensions of 12×12×1.2 mm. Figure 1 shows the design of the proposed mmWave antenna that works in two different bands. This design has modified H slots inserted into the center of the metallic patch. As the SIW design usually acts in basic mode, the calculation for the cutoff frequency f_c can be reduced to:

$$f_c = \frac{c}{2a} \tag{1}$$

where c is the speed of light within the waveguide and a is the larger internal dimension of the waveguide. The width of the dielectric field waveguide a_d is given by:

$$a_d = \frac{a}{\sqrt{\varepsilon_r}} \tag{2}$$

where ε_r is the relative permittivity of the substrate. For SIW the distance between the rows is given by:

$$W_{siw} = a_d + \frac{D^2}{0.95S} \tag{3}$$

The following equations control the radiation loss and return loss for the distance separation (S) and diameter (D).

$$\lambda_g = \frac{c}{f\sqrt{\varepsilon_r}} \tag{4}$$

$$D \leq \frac{\lambda_g}{5} \tag{5}$$

$$S \leq 2D \tag{6}$$

Metalized vias or holes are incorporated to create an SIW structure. Each metalized via or hole has a diameter of 0.5 mm.

Modified H-slots are carved into the SIW cavity's metallic plane to enhance the antenna function. The distance between the sides of the H-slot is 2.2 mm. The dimensions in the slot are indicated by the letters GW for width and GL for length. Similarly, $L2$ for length and $W2$ for width represent the parameters in the slot.

(a)

(b)

(c)

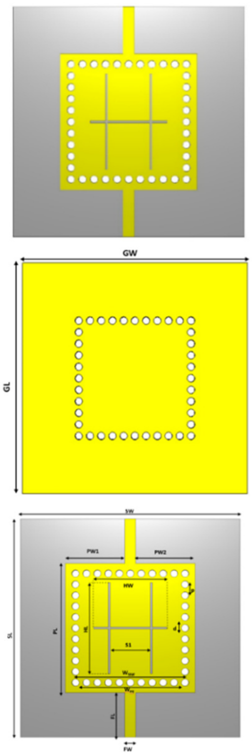

Fig. 1. Proposed modified H-slot Dual Feed Micro Strip Antenna with SIW Configuration (DFH-SIW): (a) top view, (b) back view, (c) DHF-SIW.

A 50 Ω proximity-feed microstrip line with FL length and FW width is fed to the antenna, positioned on the other side of the substrate. Between the SIW structure and the feed line lies a transitional area, with width and length indicated by Wt and Lt, respectively. The proposed values for the antenna diameter (d) and the distance (D) between the two vias are 0.5 mm and 1.0 mm, respectively. As a result, this design satisfies the requirement $D/d < 2.5$. The basic form structure shown in Figure 1 is made up of two columns that serve as vias at both edges of the structure to block signal transmission through the patch's margins, particularly when mmWave frequency loss increases relative to lower frequency. Table I displays the dimensions of the proposed antenna.

TABLE I. DIMENSIONS OF THE PROPOSED ANTENNA

Dimension	**Value (mm)**	**Dimension**	**Value (mm)**	**Dimension**	**Value (mm)**
GW, SW	12	*FW*	0.6	*Ht*	0.1
GL, SL	12	*PW1, PW2*	3.25	*SW*	0.508
PL	7.10	*HL*	5	*w*	5.80
PW	7.10	*HW*	4	*d*	0.6
FL	2.45	*S1*	2.20	*a*	0.4

III. DISCUSSION BASED ON PARAMETRIC STUDIES

Figure 2 shows three different prototypes designed with modified H-slots and SIW with different alignments of vias. For the dual-band antenna, the loss is controlled by adjusting the distance between the vias and their alignment in the antenna with respect to the dual feed line. As the distance between the vias decreases, the loss gradually decreases, since some portion of the electric field is reflected around the top of the edges of the vias and the patch of the antenna, while the remaining electric field will be removed to create unwanted distortion, as shown in DFH-SIW-V and DFH-SIW-H in Figure 2(a,b), respectively.

(a)

(b)

(c)

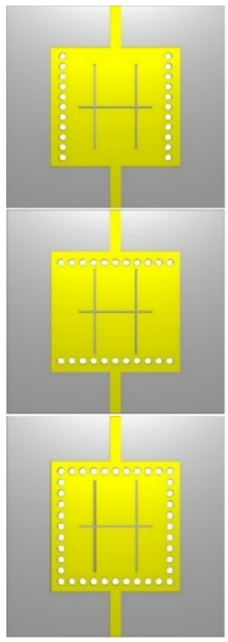

Fig. 2. Iterations of SIW vias alignment: (a) DFH-SIW-V, (b) DFH-SIW-H, (c) proposed DFH-SIW-ALL.

The proposed antennas radiate at 28 and 38 GHz because the distance between the dual feed lines and the H-slots determines the radiation pattern. The H-slot is positioned evenly in the middle of the antenna to maintain the beam's angle at zero degrees and guarantee that it focuses on the targeted substrate. Due to its size and via alignment, the proposed DFH-SIW-ALL emits radiation at 28 GHz and 38 GHz with decreased path loss. Because the H-slot is located closer to the two-sided vias in DFH-SIW-ALL, it has a stronger effect on radiation. This indicates that it is situated closer to the red zone, which is the primary surface current. Furthermore, as shown in Figure 3(a), the proposed DHF-SIW-ALL offered a greater return loss and a broad bandwidth. The proposed DFH-SIW-ALL antenna design resonates at 28/38 GHz with its best reflection coefficient parameters of -56.8 and 18.5 dB. In general, the length and width of the dielectric create huge impacts on the top band. However, the proposed antenna was designed using a modified H-slot, in which the length (HL), width (HW), and spacing of the H-slot create the greatest impact in both the resonating frequency bands. The H-slot length, width, and spacing were determined by several iterations in a software simulator to achieve the targeted resonance, as shown in Figure 3(b, c, d). The antenna slot length, width, and spacing were studied for various dimensions, and the SIW-fed DRA reflection coefficient was measured. The best coupling value was determined by observing how it varied for different dimensions.

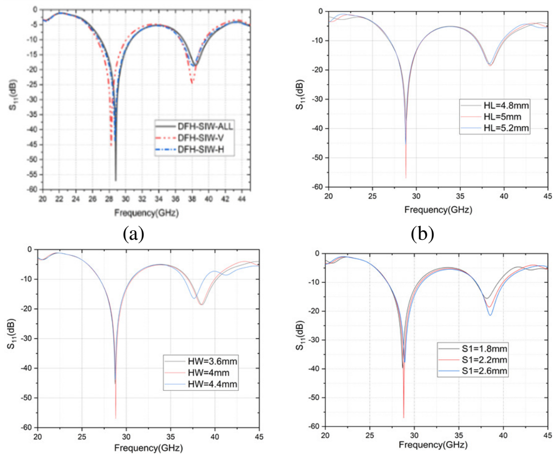

(a) (b) (c) (d)

Fig. 3. Performance analysis of return loss (S11) based on: (a) SIW structure depended on vias alignment, (b) modified H-slot length, (c) modified H-slot width, (d) modified H-slot spacing.

The results shown in Figure 3(a) provide the optimal SIW vias alignment and Figure 3(b, c, d) provides the optimal length (*HL*), width (*HW*), and spacing (*S*1) values for the proposed DFH-SIW-ALL for the optimal operating frequency band at 28/38 GHz. In Figure 3(b), it is apparent that a 5 mm slot length provides better impedance matching and a maximum return loss value. Figure 3(c) shows that the proposed design underwent various iterations by changing the width HW, indicating that changing the width shifts the top frequency band. The return loss of the proposed antenna design at both resonating frequencies is controlled by the spacing (*S*1), as shown in Figure 3(d), indicating that *S*1 = 2.2 mm achieved the optimal frequencies at both bands.

IV. SIMULATION AND FABRICATION RESULTS

Figure 4(a) shows a fabricated prototype for the DFH-SIW-ALL antenna design through a PCB process. Good impedance matching was established for the 28 and 38 GHz bands according to both the simulated and measured results. The antenna has two ports that act as feeders.

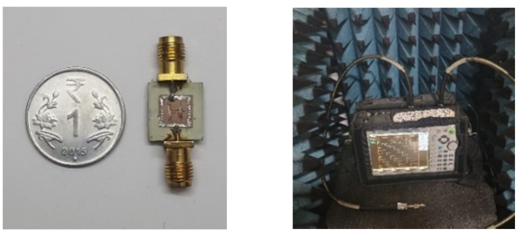

(a) (b)

Fig. 4. (a) Fabricated prototype, (b) Measurement of the scattering parameter vector analyzer.

Figure 5 shows a comparison between the simulated and measured reflection coefficients of the DHF-SIW-ALL antenna structure. Because of the effective vias alignment in the proposed antenna structure, a return loss of less than -10 dB over higher frequency and suitable optimal bandwidth are attained. At 28/38 GHz, the S11 remained below -10 dB, as shown by both simulated and experimental results.

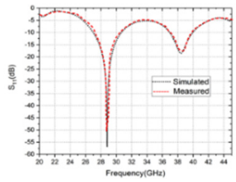

Fig. 5. Frequency response of measured return loss S11.

Figure 6 shows the actual module's measured efficiency and gain performance. When the line represents the curve fitting result, the module's measured gains exhibit frequency dependence ranging from -180° to 180°. The SIW antenna yielded gains of 6.7 dB at 38 GHz and 4.3 dB at 28 GHz, with the fitting curve's middle frequency being roughly 28 GHz. According to the simulation findings shown in Table II, produced by the CST program, the proposed model can achieve dual-band mmWave functionality and is appropriate for use in 5G applications.

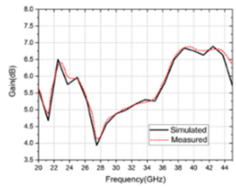

Fig. 6. Measured and simulated gain.

Figure 7 shows the simulated and measured E-plane and H-plane radiation patterns at 28/38 GHz.

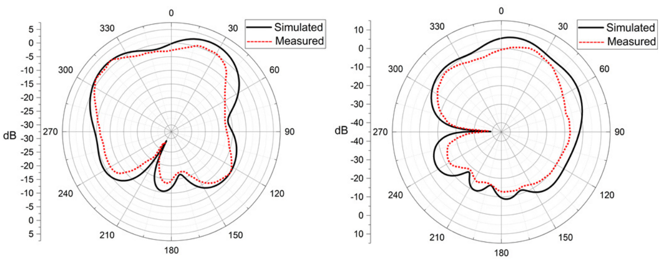

(a) (b)

Fig. 7. Measured and simulated radiation pattern for E-plane: (a) 28GHz, (b) 38GHz.

Figure 8 compares the simulated and measured radiation patterns in the E-plane and H-plane, which originate from the 38 GHz radiation of the H-slot. It is possible to note the primary beam's form from 2D (polar) radiation. This is one of the prerequisites for 5G applications. One resonant mode with two perturbed fields is excited within the SIW because of the equal H-slot lengths. Vias positioned closer to the feeders radiated at 28/38 GHz, whereas the longer H-slot radiated at the same frequency. The upper surface current distribution of the antenna at two resonant frequencies provides a better understanding of these events.

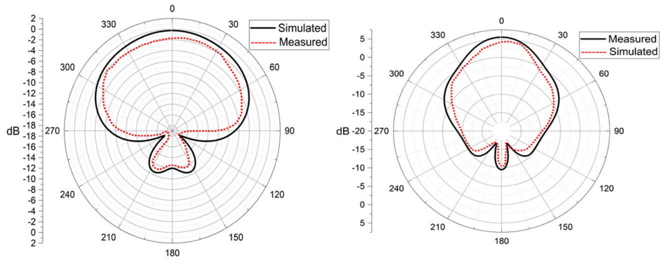

(a) (b)

Fig. 8. Measured and simulated radiation pattern for H-plane: (a) 28 GHz, (b) 38 GHz.

Table II shows the proposed antenna's simulation and experimental results. Due to SIW vias alignment and dual feed mechanism, the proposed DFH-SIW-ALL antenna had a maximum measured bandwidth of 3.7 GHz and 3.23 GHz at the operating frequencies of 28/38 GHz, as well as a high return loss of -51.2 dB and -18.2 dB, respectively. With a straightforward modified slotted design, the proposed antenna measured high gains of 4.1 dB and 6.56 dB at operating frequencies of 28 and 38 GHz, respectively. Table III compares the proposed design with existing dual-band mmWave antennas.

TABLE II. MEASURED AND SIMULATION RESULTS FOR THE PROPOSED DFH-SIW-ALL ANTENNA

Parameters	Results	28 GHz	38 GHz
Bandwidth (GHz)	Simulated	3.7	3.23
	Measured	3.64	3.12
Gain (dB)	Simulated	4.3	6.7
	Measured	4.1	6.56
S11 (dB)	Simulated	-56.9	-18.5
	Measured.	-51.2	-18.2

TABLE III. COMPARISON BETWEEN PROPOSED AND EXISTING DUAL-BAND MMWAVE ANTENNAS

Ref/model	Center frequency (GHz)	Return loss (dB)	Bandwidth (GHz)	Gain (dB)
[6]	26	-16	2.8	8.8
	28	-19	0.6	8.03
[11]	28	-27	1.6	4.6
	38	-33	2	4.8
[12]	28	-34.5	1.23	6.6
	38	-27.3	1.06	5.86
[13]	28	-24.4	2.6	4.8
	38	-15.8	2.3	4.6
[15]	28	-19	1.6	5.4
	38	-24	2.75	4.2
DFH-SIW-V	28	-45.7	3.5	4.19
	38	-24.48	2.91	6.39
DFH-SIW-H	28	-43.72	3.2	4.23
	38	-18.8	2.987	6.38
Proposed DFH-SIW-ALL	28	-56.9	3.7	4.3
	38	-18.5	3.23	6.7

The results show that at operating frequencies of 28 and 38 GHz, the proposed DHF-SIW-ALL antenna offers ideal return loss with improved gain and optimal bandwidth, compared with the dual-band antennas proposed in [6, 11-13, 15]. The mmWave 5G communications are very important. As relatively broad bandwidths are available at 28 and 38 GHz, the proposed antenna provides a higher data capacity. To feed a mmWave antenna, waveguide structures are particularly suitable due to low loss and high power handling capability. Since the proposed antenna offers a wide bandwidth, high gain, and effective return loss at 28 and 38 GHz, it is proposed for prospective 5G wireless networks in the future.

IV. CONCLUSION

This study proposed a simple dual-feed, dual-band, single-element SIW antenna with a modified H-slot. The proposed antenna, DFH-SIW-ALL, has three distinct features. First, it has a compact design with single-layer construction that provides direct and easy integration. Second, to counteract path loss, the antenna uses impedance-matching gaps with a modified H-slot to control the antenna resonance in the lower and higher frequency bands. Third, the unique SIW vias structure was created with a dual-feed mechanism to provide optimal gain and wider bandwidth. Other dual-band SIW antennas had narrow bandwidth, while the proposed antenna has wide bandwidth with optimal gain, which is essential for maintaining high data rates in mmWave applications. The proposed antenna has a sufficient radiation pattern, and optimal impedance bandwidth and gain when operating at 28/38 GHz. The single element, having operating bandwidths of 3.7 GHz and 3.23 GHz, realized 4.3 dBi and 6.7 dBi gain for the 28 and 38 GHz bands, respectively. Due to its excellent performance, the proposed SIW antenna is recommended for 5G Ka-band applications. Compared to the lower band, the higher band of the proposed antenna has a narrower bandwidth and reduced return loss. SIW with integrated DRAs will be used in 5G technologies in the future. When SIW and DRA are used together, a dual-band antenna design can achieve several beneficial features, such as minimal signal attenuation, wide bandwidth, and streamlined manufacturing procedures.

ACKNOWLEDGMENT

The authors acknowledge the DST through technical support from SR/PURSE/2023/196 and SR/FST/ET-II/2019/450.

REFERENCES

[1] M. J. Hakeem and M. M. Nahas, "Improving the Performance of a Microstrip Antenna by Adding a Slot into Different Patch Designs," *Engineering, Technology & Applied Science Research*, vol. 11, no. 4, pp. 7469–7476, Aug. 2021, https://doi.org/10.48084/etasr.4280.

[2] M. Nahas, "A Super High Gain L-Slotted Microstrip Patch Antenna For 5G Mobile Systems Operating at 26 and 28 GHz," *Engineering, Technology & Applied Science Research*, vol. 12, no. 1, pp. 8053–8057, Feb. 2022, https://doi.org/10.48084/etasr.4657.

[3] P. Bora, P. Pokkunuri, and B. T. P. Madhav, "The Design of Closed Square RR Loaded 2-Port MIMO for Dual Band Applications," *Engineering, Technology & Applied Science Research*, vol. 12, no. 2, pp. 8382–8387, Apr. 2022, https://doi.org/10.48084/etasr.4760.

[4] X. Zhang, Y. Chen, Y. Xie, and L. Liu, "An Improved E-Plane Waveguide Power Divider Design for 94GHz Dual-Pyramidal Horn

Antenna," *Applied Computational Electromagnetics Society Journal*, vol. 34, no. 12, 2019.

[5] Y. M. Hussain, M. K. A. Rahim, N. A. Murad, H. O. Hanoosh, and H. H. Keriee, "Substrate Integrated Waveguide Cavity slot Antenna at millimeter wave for 5G application," in *2021 International Symposium on Antennas and Propagation (ISAP)*, 2021.

[6] Y. M. Hussein, M. K. A. Rahim, N. A. Murad, H. O. Hanoosh, and N. B. M. Nadzir, "Substrate Integrated Waveguide Antenna at Millimeter Wave for 5G Application," *The Applied Computational Electromagnetics Society Journal (ACES)*, vol. 37, no. 4, pp. 478–484, Apr. 2022, https://doi.org/10.13052/2022.ACES.J.370413.

[7] H. O. Hanoosh, M. K. A. Rahim, N. A. Murad, and Y. M. Hussein, "Multi-beams waveguide slot antennas at X-band for wireless communications systems," *Applied Computational Electromagnetics Society Journal*, vol. 35, no. 7, pp. 797–802, 2020.

[8] P. M. Mpele, F. M. Mbango, and D. B. O. Konditi, "A Small Dual Band (28/38 GHz) Elliptical Antenna For 5G Applications With DGS," *International Journal of Scientific & Technology Research*, vol. 8, no. 10, pp. 353–357, 2019.

[9] Y. Cheng and Y. Dong, "Dual Circularly Polarized Broadband Antenna Array for Millimeter-Wave Applications," *IEEE Antennas and Wireless Propagation Letters*, vol. 21, no. 12, pp. 2377–2381, Dec. 2022, https://doi.org/10.1109/LAWP.2022.3193940.

[10] L. X. Cui, X. H. Ding, W. W. Yang, L. Guo, L. H. Zhou, and J. X. Chen, "Communication Compact Dual-Band Hybrid Dielectric Resonator Antenna for 5G Millimeter-Wave Applications," *IEEE Transactions on Antennas and Propagation*, vol. 71, pp. 1005–1010, Jan. 2023, https://doi.org/10.1109/TAP.2022.3211389.

[11] T. Deckmyn, M. Cauwe, D. Vande Ginste, H. Rogier, and S. Agneessens, "Dual-Band (28,38) GHz Coupled Quarter-Mode Substrate-Integrated Waveguide Antenna Array for Next-Generation Wireless Systems," *IEEE Transactions on Antennas and Propagation*, vol. 67, pp. 2405–2412, Apr. 2019, https://doi.org/10.1109/TAP.2019.2894325.

[12] A. E. Farahat and K. F. A. Hussein, "Dual-Band (28/38 GHz) Wideband MIMO Antenna for 5G Mobile Applications," *IEEE Access*, vol. 10, pp. 32213–32223, 2022, https://doi.org/10.1109/ACCESS.2022.3160724.

[13] I. J. Hwang, J. I. Oh, H. W. Jo, K. S. Kim, J. W. Yu, and D. J. Lee, "28 GHz and 38 GHz Dual-Band Vertically Stacked Dipole Antennas on Flexible Liquid Crystal Polymer Substrates for Millimeter-Wave 5G Cellular Handsets," *IEEE Transactions on Antennas and Propagation*, vol. 70, pp. 3223–3236, May 2022, https://doi.org/10.1109/TAP.2021.3137234.

[14] L. Yan, W. Hong, K. Wu, and T. J. Cui, "Investigations on the propagation characteristics of the substrate integrated waveguide based on the method of lines," *IEE Proceedings - Microwaves, Antennas and Propagation*, vol. 152, no. 1, pp. 35–42, Feb. 2005, https://doi.org/10.1049/ip-map:20040726.

[15] B. A. F. Esmail and S. Koziel, "Design and Optimization of Metamaterial-Based Dual-Band 28/38 GHz 5G MIMO Antenna With Modified Ground for Isolation and Bandwidth Improvement," *IEEE Antennas and Wireless Propagation Letters*, vol. 22, pp. 1069–1073, May 2023, https://doi.org/10.1109/LAWP.2022.3232622.

[16] R. A. Saravanan, B. T. P. Madhav, P. Pardhasaradhi, G. S. Rao, and N. Prasad, "A High Gain Dual Feed Microstrip Patch Antenna with Modified H-Slot for Ka-Band (28/38 GHz) Application.," *International Journal of Microwave & Optical Technology*, vol. 19, no. 2, 2024.

[17] P. Kumawat and S. Joshi, "Review of slotted SIW antenna at 28 GHz and 38 GHz for mm-wave applications," in *2020 12th International Conference on Computational Intelligence and Communication Networks (CICN)*, 2020, pp. 8–13.

[18] K. Wu, Y. J. Cheng, T. Djerafi, and W. Hong, "Substrate-Integrated Millimeter-Wave and Terahertz Antenna Technology," *Proceedings of the IEEE*, vol. 100, no. 7, pp. 2219–2232, May 2012, https://doi.org/10.1109/JPROC.2012.2190252.

[19] M. Bozzi, A. Georgiadis, and K. Wu, "Review of substrate-integrated waveguide circuits and antennas," *IET Microwaves, Antennas & Propagation*, vol. 5, no. 8, pp. 909–920, Jun. 2011, https://doi.org/10.1049/iet-map.2010.0463.

[20] T. Hong, Z. Zhao, W. Jiang, S. Xia, Y. Liu, and S. Gong, "Dual-Band SIW Cavity-Backed Slot Array Using TM020 and TM120 Modes for 5G Applications," *IEEE Transactions on Antennas and Propagation*, vol. 67, no. 5, pp. 3490–3495, Feb. 2019, https://doi.org/10.1109/TAP.2019.2900394.

[21] Q. J. Deng, Y. M. Pan, X. Y. Liu, and K. W. Leung, "A Singly-Fed Dual-Band Aperture-Sharing SIW Cavity-Backed Slot Antenna With Large Frequency Ratio," *IEEE Transactions on Antennas and Propagation*, vol. 71, no. 2, pp. 1971–1976, Oct. 2023, https://doi.org/10.1109/TAP.2022.3232208.